immunohistochemically stained (e.g., with dysferlin or dystrophin) to exclude other suspected disorders.

Immunofluorescence double staining for CD8 and MHC-1

Frozen biopsied muscle specimens from all patients were cut into 7-μm-thick sections, placed on aminosilane-coated slides and dried at room temperature. Sections were blocked with 10% normal goat serum in phosphate-buffered saline and then incubated with a mixture of mouse antihuman CD8 monoclonal antibody (diluted 1:50, isotype IgG1; Dako, Glostrup, Denmark) and mouse antihuman HLA-ABC antigen monoclonal antibody (diluted 1:50 isotype IgG2a; Dako) for 12 h at 4°C. Then, an isotype-specific goat antimouse antibody mixture (goat antimouse IgG1 Alexa Fluor 594 and goat antimouse IgG2a Alexa Fluor 488 to detect CD8 and HLA-ABC antigens, respectively; Invitrogen, Carlsbad, CA, USA) was applied for 60 min at room temperature. Sections were counterstained with 4',6-diamino-2-phenylindole. Signals were collected by a confocal laser scanning microscope (FV500; Olympus, Tokyo, Japan). The fluorescence of individual fluorochromes was captured sequentially.

Polymerase chain reaction

Polymerase chain reaction (PCR) was carried out in a Gene Amp PCR system 9700 (GeneAmp® Applied Biosystems, Singapore) to determine HTLV-1 positivity using 5 μL of DNA (10 μg/mL) extracted from fresh frozen muscle tissue as a template with 20 μL of PCR mixture containing primers specific to the HTLV-1 pX region. Products were analyzed by electrophoresis using agarose gel, as described previously.[10]

The PCR products of samples that were not proven to be HTLV-1-positive were subjected to a second PCR under the same conditions and re-analyzed by electrophoresis using agarose gel. Samples that proved to be HTLV-1-positive after the second PCR were considered positive; samples that were HTLV-1-negative were subjected to the first PCR again, and the total amount of first PCR products (25 μL) was subjected to a second PCR (5 μL/reaction; i.e., five PCR reactions) to avoid loss of any viral amplicons. The results were reconsidered to be either positive or negative. All experiments were carried out using positive and negative controls, and sensitivity was determined by known titrated pX amplicon solutions from 1–5000 copies·5 μL^{-1}; the detection limit of the pX was one copy/reaction. All results were confirmed three times.

Real-time PCR

All cases that proved to be HTLV-1-positive were tested for tissue proviral load using an ABI PRISM7700 sequence detector (Applied Biosystems, Tokyo, Japan) using 15 μL of DNA (10 μg/mL) extracted from fresh frozen muscle tissue as a template with β-globin as an internal control. Tissue proviral loads were calculated using the following formula: (copy number of HTLV-1 Tax/10 000 cells) = [(tax average × 2)/β-actin average] × 10 000.[11] All samples were measured in triplicate, and the average was then determined.

Serology

HTLV-1 seropositivity was examined using a particle agglutinin method (Serodia-HTLV-1; Fujirebio, Tokyo, Japan) and an enzyme-linked immunosorbent assay (Virus-Antibody EIA IgG; Denka-Seiken, Japan).

Immunohistochemistry

Frozen biopsied muscle specimens from all patients were cut into 7-μm-thick sections that were placed on aminosilane-coated slides, dried at room temperature and blocked with a blocking solution. The sections were then incubated with the following antibodies: monoclonal mouse antihuman CD4 (diluted 1:20), CD8 (diluted 1:50), CD20 (diluted 1:200) and CD68 (diluted 1:100; all obtained from Dako); neural cell adhesion molecule (NCAM; diluted 1:10; BD, Franklin Lakes, NJ, USA); myosin heavy chain (neonatal; MHCn; diluted 1:10; Novocastra, Newcastle, UK); perforin (diluted 1:25; PharmaCell, Paris, France); thrombomodulin (TM; diluted 1:50; Dako); and heat shock protein 47 (HSP47; diluted 1:50; Santa Cruz Biotechnology, Santa Cruz, CA, USA). Sections were incubated with each antibody for 12 h at 4°C. Antimouse antibodies were subsequently applied for 30 min at room temperature. Finally, the sections were visualized using the DAB (brown color) or DAKO AEC systems (red color) after setting positive and negative controls using mouse IgG negative control as a first antibody (Dako). Three control muscle biopsies that were HTLV-1-negative and had minimal pathological changes were also investigated.

Quantitative analysis of histopathological findings

Necrotic fibers, as well as all histochemical and immunohistochemical stains, were subjected to quantitative analysis. Samples (at least three sections from

© 2011 Japanese Society for Neuroimmunology

each sample) were examined at five fields (×200 magnification) selected randomly in a zigzag manner to avoid overlapping of the fields or recounting the same fibers. More than 200 fibers in each field were counted and all examined fields were averaged.

Each cellular subset and the total number of endomysial and perimysial infiltrating inflammatory cells were counted in at least three sections from each specimen at five different fields (×200 magnification) selected randomly in a zigzag manner; the mean ratio of the total number of infiltrating inflammatory cells and each cellular subset was evaluated in all specimens of both groups.

Electron microscopy

Several epon-embedded tissue blocks from each of the seven HTLV-1-positive patients, five HTLV-1-negative PM patients and three normal control specimens were examined. Tissue blocks were fixed overnight in 3% glutaraldehyde, postfixed in 1% osmium tetroxide in 0.05 mol/L cacodylate buffer (pH 7.3), and dehydrated in graded alcohol. Semi-thin sections were stained with toluidine blue and safranin, and examined by light microscopy. Areas with inflammatory infiltrates and variable-sized fibers that were well fixed and free of preparation artifacts were selected for electron microscopy. Ultrathin sections were stained with uranyl acetate and lead citrate, and examined using an H-7100 electron microscope (Hitachi High-Technologies, Hitachinaka, Ibaraki, Japan). At least three tissue blocks from each specimen were cut, and at least three sections from each block were examined; five adjacent fibers in each field from five fields (×200 magnification) selected randomly in a zigzag manner from each section were examined. More than 100 mitochondria in each fiber were counted, and the percentage was determined.

Statistical analysis

All quantitative data were analyzed for descriptive statistics and by the Mann–Whitney *U*-test and Spearman's rank correlation test using StatView software version 5.0.1. (SAS Institute Inc, Cary, NC, USA).

Data are presented as means (SD). *P*-values <0.05 were considered significant.

Results

Patient selection

Of the 68 patients reported to have inflammatory myopathy who had undergone a biopsy over the past 10 years, we carefully selected 21 patients with myositis not associated with skin lesions or any other diseases. Patients who reported to have dermatomyositis ($n = 14$), IBM ($n = 12$), inflammatory myopathy associated with HAM/TSP ($n = 11$) and inflammatory myopathy associated with other diseases ($n = 10$) were excluded from analysis on the basis of clinical and pathological criteria. The selection process and diagnoses of the excluded patients are shown in Fig. 1.

The 21 selected patients had the following common features: (i) subacute bilateral symmetrical progressive weakness commencing in adulthood and involving proximal muscles more than distal; (ii) elevated serum CK more than twice the normal level (normal range 26–140 IU/L); (iii) myopathic findings in EMG; and (iv) muscle biopsy findings (Fig. 2a–d,f) with inflammatory cell infiltration, CD8 cells surrounding healthy intact non-necrotic fibers as well as myopathic changes, such as variations in muscle fiber size, necrosis, degeneration and regeneration without rimmed vacuoles. In addition, the clinical course and manifestations of these 21 patients were retrospectively investigated to ensure a satisfactory response to steroid therapy with improvements in their symptoms (e.g., muscle tone, weakness and fatigue while walking, and lowered CK levels) and to confirm the diagnosis of PM.[12,13]

On re-evaluating the 21 selected PM patients using the modified criteria introduced by Dalakas and Hohlfeld,[7] the CD8/MHC-1 complex was detected in six patients (29%; Fig. 3a–c) who were diagnosed with definite PM. The remaining 15 patients showed MHC-1 expression and infiltration of CD8+ cells, but the CD8/MHC-1 complex was not detected; these patients were diagnosed with probable PM (Fig. 3d,f).

Confirmation of HTLV-1 positivity by nested PCR and proviral loads of HTLV-1-positive cases

Nested PCR carried out using DNA extracted from fresh frozen muscle biopsies showed that among the 21 patients with PM, 11 and 10 were HTLV-1-positive and HTLV-1-negative, respectively. PCR positivity for HTLV-1 strongly corresponded to seropositivity for HTLV-1. Although tissue proviral loads of HTLV-1 ranged from 1 to 2063 (1 copy/10^4 cells), the proviral loads were not correlated with any examined clinical or histopathological values using Spearman's rank correlation test (data not shown).

The six patients expressing the CD8/MHC-1 complex included three from the HTLV-1 positive group

© 2011 Japanese Society for Neuroimmunology

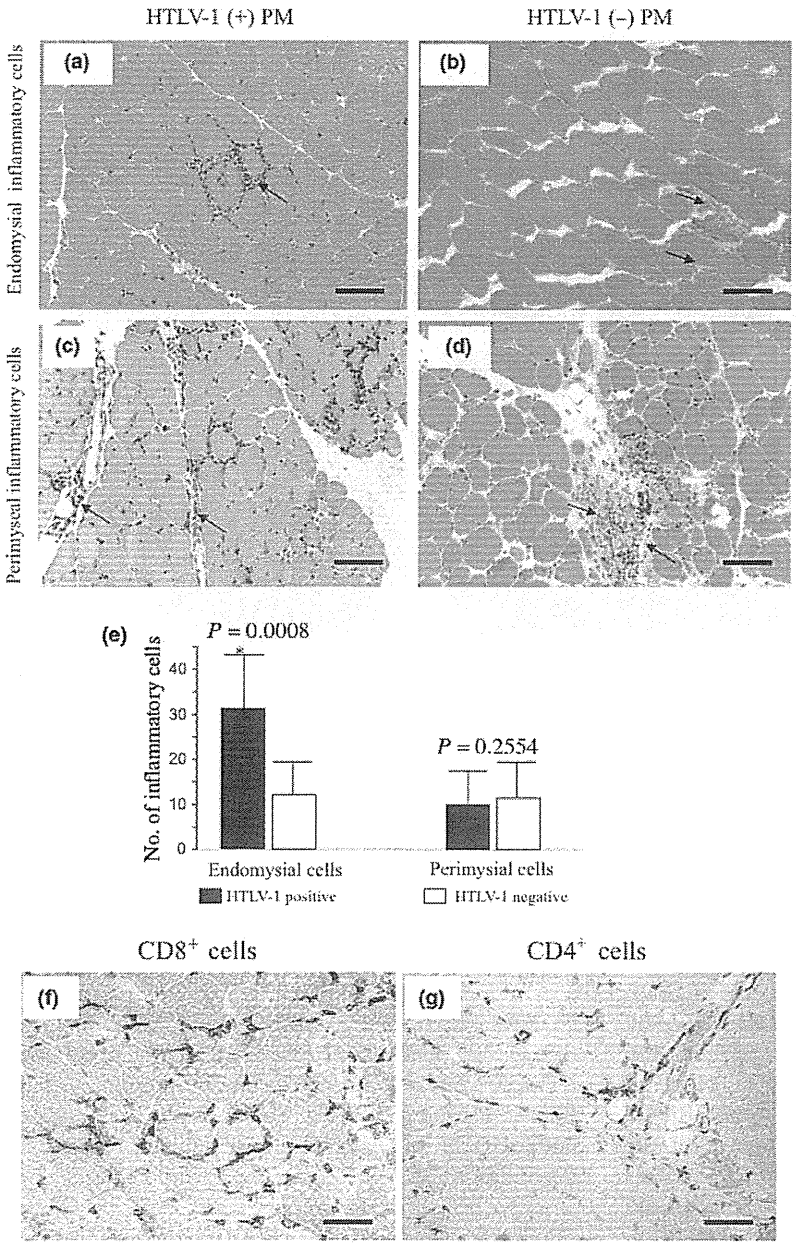

Figure 2 Distribution and subsets of inflammatory cells in cross-sections of muscles biopsied from human T-lymphotropic virus type 1 (HTLV-1)-positive and HTLV-1-negative polymyositis (PM) patients. (a) Abundant endomysial inflammatory cells in HTLV-1-positive PM (arrow). (b) Infrequent endomysial inflammatory cells in HTLV-1-negative PM (arrows). (c,d) Equal numbers of perimysial inflammatory cells in HTLV-1-positive and HTLV-1-negative PM (arrows). Bars (a)–(d) 100 μm. (e) Combined data for all study patients. Significantly greater numbers of endomysial inflammatory cells in HTLV-1-positive PM (P = 0.0008; Mann–Whitney U-test). Immunohistochemistry for (f) $CD8^+$ (bar, 50 μm) and (g) $CD4^+$ (bar, 100 μm) cells shows that they are predominant in the endomysium and perimysium, respectively.

(3/11, 27%) and three from the HTLV-1-negative group (3/10, 30%).

Clinical and laboratory differences

Detailed clinical and laboratory data are shown in Table 1. There were no significant differences between groups regarding age, sex or serum CK levels. However, the duration of illness from the onset of symptoms to biopsy was significantly longer in HTLV-1-positive PM patients [range 1–240 months; mean 66 months (73.6)] compared with that in HTLV-1-negative PM patients [range 1–24 months; mean 8 months (6.9); P = 0.0043].

Endomysial inflammatory cells are more frequent in HTLV-1-positive PM

Routine examination showed typical histopathological findings of PM in all patients. However, there were significantly more endomysial inflammatory cells in HTLV-1-positive PM patients [range

© 2011 Japanese Society for Neuroimmunology

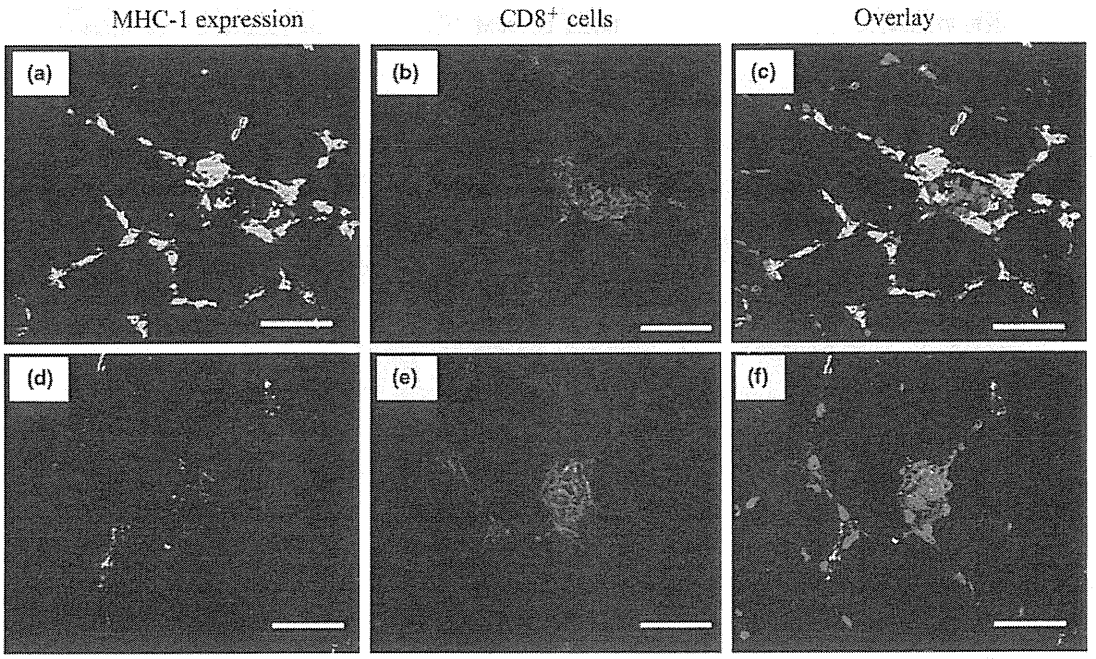

Figure 3 Detection of the CD8/MHC-1 complex by double staining for MHC-1 and CD8 antigens by immunofluorescence. (a) Histologically healthy non-necrotic fibers expressing histocompatibility complex (MHC)-1antigens (green color). (b) $CD8^+$ cells surrounding and invading histologically healthy non-necrotic muscle fibers (red color). (c) Overlay of both histologically healthy non-necrotic fibers expressing MHC-1 antigens (green color) and $CD8^+$ cells invading them (red color). (d) Histologically healthy non-necrotic fibers not expressing MHC-1 antigens (no green color). (e) $CD8^+$ cells surrounding and invading the histologically healthy non-necrotic muscle fibers (red color). (f) Overlay of both histologically healthy non-necrotic fibers not expressing MHC-1 antigens (no green color) and $CD8^+$ cells invading them (red color). Bars, 100 μm.

5–50 cells/×200 field (F); mean 31 (13.7)/F] compared with HTLV-1-negative PM patients [range 3–27 cells/F; mean 11 (8.6)/F; $P = 0.0008$; Fig. 2a,b,e]. There was no significant difference between the number of perimysial inflammatory cells in the HTLV-1-positive PM [range 0–27 cells/F; mean 9 (8.2)/F] and HTLV-1-negative PM groups [range 5–25/F; mean 11 (6.4)/F; Fig. 2c–e]. Regarding the subsets of inflammatory infiltrates, $CD8^+$ and $CD4^+$ cells were predominant in the endomysium and perimysium in both groups, respectively (Fig. 2f,g). The subsets of infiltrating $CD4^+$, $CD8^+$, $CD68^+$ and $CD20^+$ cells in the endomysium were 30%, 46%, 21% and 3%, in the HTLV-1-positive PM group, and 31%, 48%, 19% and 2% in the HTLV-1-negative PM group, respectively. The subsets of infiltrating $CD4^+$, $CD8^+$, $CD68^+$ and $CD20^+$ cells in the perimysium were 48%, 37%, 14% and 1% in the HTLV-1-positive PM group, and 44%, 37%, 16% and 3% in the HTLV-1-negative PM group, respectively. There were no apparent differences in the subsets of infiltrating cells between the two groups.

Necrotic fibers are less common in HTLV-1-positive patients

Necrotic fibers, which were counted and averaged out of 200 fibers, were less frequently observed in HTLV-1-positive patients [Fig. 4a; range 0–4/200 fibers; mean 2 (1.75)] than in HTLV-1-negative patients [Fig. 4b; range 1–25/200 fibers; mean 6 (7); $P = 0.0201$; Fig. 4c].

Regenerative activity is more common in HTLV-1-positive PM

The number of fibers expressing regenerative activity was determined using anti-NCAM and anti-MHCn antibodies. NCAM-positive fibers tended to be more common in HTLV-1-positive PM [Fig. 5a; range 2–25/200 fibers; mean 10 (8.1)] than in HTLV-1-negative PM [Fig. 5b; range 0–20/200 fibers; mean 6 (5.8)]; $P = 0.063$; Fig. 5e). MHCn-positive staining fibers, which are a more specific regenerative marker, were significantly more common in HTLV-1-positive PM [Fig. 5c; range 3–25/200 fibers; mean 11

© 2011 Japanese Society for Neuroimmunology

Table 1 Detailed clinical and laboratory data of all 21 patients

Case serial number	Age/sex	Duration of illness (months)	Laboratory data: Tissue nested PCR	Serum anti HTLV-1 antibodies	Tissue viral preload (copy/10^4 cells)	CK (IU/L)	Anti jo-1	ANA	Muscle weakness	Gait	EMG	Response to CS treatment	Site of biopsy
Po 1	50/F	120	+	+	1	400	–	–	Moderate S P > D	D	Myopathic	Effective	Biceps brachii
Po 2	59/F	12	+	+	1627	1390	–	–	Mild S P > D	N	Myopathic	Effective	Biceps brachii
Po 3	59/F	12	+	+	1	1100	–	–	Moderate S P > D	D	Myopathic	Effective	Biceps brachii
Po 4	56/F	24	+	+	4	370	–	–	Moderate S P > D	M	Myopathic	Effective	Biceps brachii
Po 5	63/F	24	+	+	316	1538	–	–	Mild S P > D	M	Myopathic	Effective	Biceps brachii
Po 6	62/F	144	+	+	7	349	–	–	Mild S P > D	M	Myopathic	Effective	Biceps brachii
Po 7	53/M	1	+	+	633	4742	–	–	Mild S P > D	N	Myopathic	Effective	Biceps brachii
Po 8	66/M	48	+	+	7	2924	+	–	Mild S P > D	M	Myopathic	Effective	Biceps brachii
Po 9	51/F	60	+	+	1	206	–	–	Moderate S P > D	D	Myopathic	Effective	Biceps brachii
Po 10	70/M	240	+	+	2063	355	–	–	Mild S P > D	M	Myopathic	Effective	Quadriceps femoris
Po 11	35/F	36	+	+	13	4000	–	–	Moderate S P > D	D	Myopathic	Effective	Biceps brachii
Neg 1	53/F	24	–	–	NA	599	–	–	Moderate S P > D	D	Myopathic	Effective	Biceps brachii
Neg 2	65/F	8	–	–	NA	2400	–	–	Moderate S P > D	D	Myopathic	Effective	Biceps brachii
Neg 3	57/F	12	–	–	NA	4525	–	–	Mild S P > D	M	Myopathic	Effective	Biceps brachii
Neg 4	60/F	12	–	–	NA	330	–	–	Moderate S P > D	D	Myopathic	Effective	Biceps brachii
Neg 5	50/F	2	–	–	NA	840	–	–	Mild S P > D	N	Myopathic	Effective	Biceps brachii
Neg 6	62/M	10	–	–	NA	523	–	–	Mild S P > D	M	Myopathic	Effective	Biceps brachii
Neg 7	36/F	2	–	–	NA	7760	–	–	Mild S P > D	N	Myopathic	Effective	Biceps brachii
Neg 8	67/F	6	–	–	NA	2895	–	–	Moderate S P > D	D	Myopathic	Effective	Biceps brachii
Neg 9	58/F	1	–	–	NA	834	–	–	Mild S P > D	N	Myopathic	Effective	Biceps brachii
Neg 10	56/M	4	–	–	NA	561	–	–	Mild S P > D	M	Myopathic	Effective	Biceps brachii

Muscle strength score: 5, normal; 4, good; 3, fair; 2, poor; 1, trace; 0, no muscle contraction. +, positive; –, negative. ANA, anti-nuclear antobody; anti jo-1, antibody antihistidyl t-RNA synthetase antibody; CK, creatine kinase; CS, corticosteroid; D, distal muscle strength; D, disturbed gait; EMG, elecromyography; HTLV-1, human T-lymphotropic virus type 1; N, normal gait; NA, not assessed; M, mildly changed gait; P, proximal muscle strength; PCR, polymerase chain reaction; S, symmetrical muscle strength.

© 2011 Japanese Society for Neuroimmunology

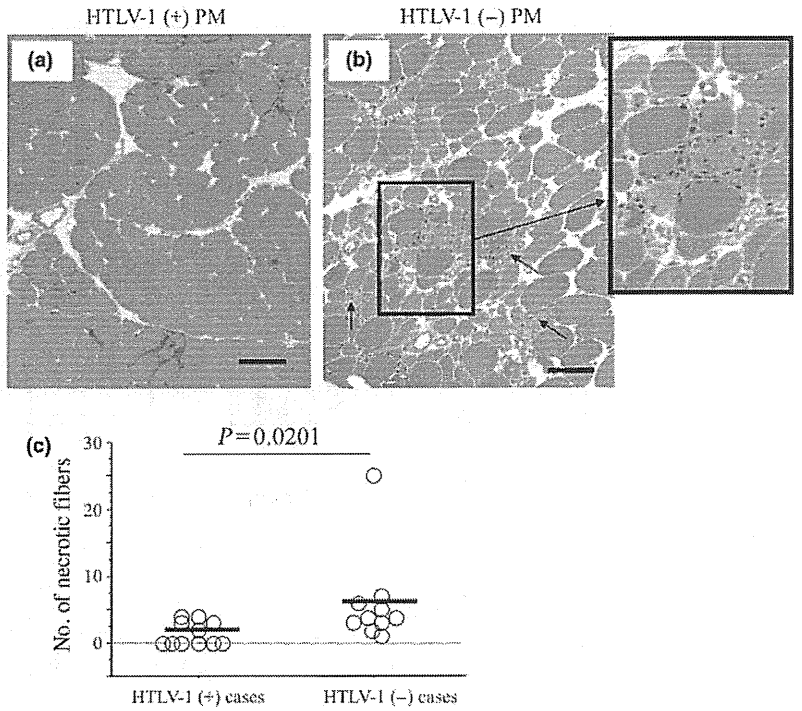

Figure 4 Necrotic fibers in cross-sections of muscles biopsied from human T-lymphotropic virus type 1 (HTLV-1)-positive and HTLV-1-negative PM patients. (a) Very few necrotic fibers are seen in HTLV-1-positive polymyositis (PM); most fibers are histologically viable and healthy. (b) A greater number of necrotic fibers are seen in HTLV-1-negative PM (arrows); inset shows higher magnification of frequently seen necrotic fibers invaded by inflammatory phagocytic cells. (c) Combined data for all study patients. Significantly greater numbers of necrotic fibers are seen in HTLV-1-negative PM than in HTLV-1-positive PM (P = 0.0201; Mann–Whitney U-test). Bars (a)–(b) 100 μm.

(8.3)] than in HTLV-1-negative PM [Fig. 5d; range 0–20/200 fibers; mean 6 (5.5); P = 0.045; Fig. 5e]. There was no apparent difference between the groups regarding the staining profiles for the other antibodies including anti-HSP47 (a marker for subsequent fibrotic processes), perforin (a cytolytic protein and a marker of apoptosis induced by $CD8^+$ and natural killer cells) and thrombomodulin, which has anti-thrombotic, anti-inflammatory and anti-apoptotic activities.

CCO activity is decreased in HTLV-1-positive PM

Using normal controls as a reference (Fig. 6a), peripheral fields were not examined to avoid dryness artifacts in the samples. The examined central fields were separated from the edges of the sections by at least one field distance. Partially decreased CCO-stained (Fig. 6c) or completely CCO-negative fibers (Fig. 6d) were frequently found in 9 of 11 HTLV-1-positive PM patients, but only in 3 of 10 HTLV-1-negative PM patients (Fig. 6b). In all 21 PM patients, the number of fibers with partially decreased CCO activity or completely CCO-negative that were counted out of 200 fibers was higher in HTLV-1-positive PM patients [range 0–28/200 fibers; mean, 7 (8)] than in HTLV-1-negative PM patients [range 0–1/200 fibers; mean 1 (1); P = 0.0031; Fig. 6e].

The staining profile of SDH enzyme histochemistry was normal in all HTLV-1-positive and HTLV-1-negative PM cases except for one case from each group that showed mild reduction in 1–2 fibers/200 fibers.

Mitochondrial morphological abnormalities in HTLV-1-positive PM

We examined semi-thin sections from seven HTLV-1-positive patients showing partially reduced CCO-staining or completely CCO-negative fibers. Sections that had areas with inflammatory infiltrates and variable-sized closely backed myofibers without artifacts and separated by a thin endomysium were selected for ultrathin sections. Morphologically abnormal mitochondria were found on examination of these ultrathin sections (range 8–61%; mean 30%). To avoid misinterpretation of preparation or fixation artifacts, we only considered abnormal mitochondria in well-fixed fields with intact surrounding sarcoplasm filled with closely packed myofibrils arranged in a precise manner without any contraction artifacts; other adjacent mitochondria showed slight swelling, but showed intact unseparated inner and outer membranes, and intact homogenous matrices and cristae. The morphologically abnormal mitochondria showed high-amplitude abnormal swelling without membrane separation, irregular or bizarre shapes, membrane disruption, matrix fragmentation, loss of cristae (Fig. 7c,e), and myelin-like structures (Fig. 7d). In

© 2011 Japanese Society for Neuroimmunology

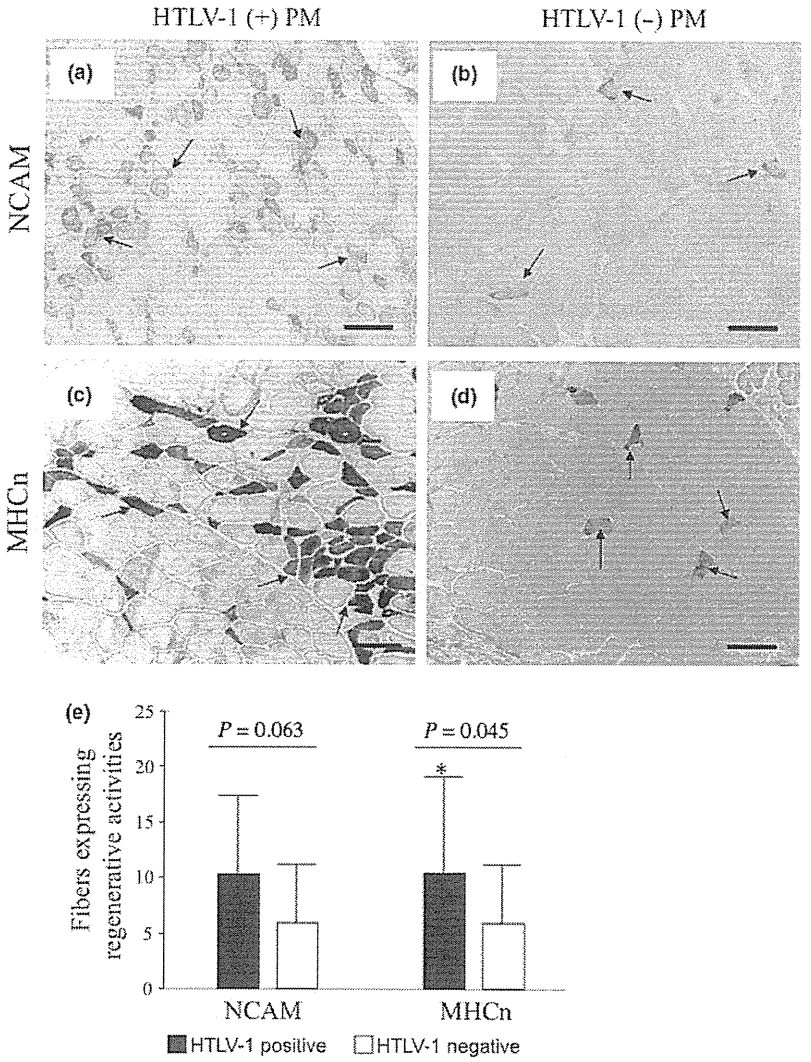

Figure 5 (a,b) Immunohistochemistry for neural cell adhesion molecule (NCAM) and (c,d) neonatal myosin heavy chain (MHCn). Myofibers show increased and decreased regenerative activity with NCAM (arrows) in (a) human T-lymphotropic virus type 1 (HTLV-1)-positive and (b) HTLV-1-negative polymyositis (PM), respectively. (c) Regenerative activity is more pronounced in HTLV-1-positive PM on MHCn staining (arrows). (d) Myofibers show decreased regenerative activity in HTLV-1-negative PM on MHCn staining (arrows). (e) Combined data for all study patients. An increase in the numbers of fibers showing regenerative activity in HTLV-1-positive PM with NCAM staining ($P = 0.063$, Mann–Whitney *U*-test) and significantly greater numbers of fibers showing regenerative activity with MHCn staining ($P = 0.045$; Mann–Whitney *U*-test) in HTLV-1-positive PM compared with HTLV-1-negative PM. Bars (a)–(d) 100 μm.

contrast, such abnormal mitochondria were not observed in normal controls or all five examined HTLV-1-negative patients (Fig. 7a,b). The percentage of mitochondria with morphological abnormalities was correlated with the number of partially reduced or completely CCO negative-stained fibers ($P = 0.0304$; Spearman's rank correlation; Fig. 7f).

Detailed histological, histochemical and electron microscopy findings in the skeletal muscle of all 21 PM patients are shown in Table 2.

Discussion

The present retrospective study included all patients with inflammatory myopathy who had undergone biopsy over the past 10 years at Kagoshima University Hospital, South Kyushu, Japan. From these patients, we selected our cohort after excluding patients with myositis associated with any other diseases or factors other than HTLV-1 that might affect our results.

On retrospective re-evaluation of all 21 selected patients using the modified criteria introduced by Dalakas and Hohlfeld,[7] six patients (29%) were diagnosed with definite PM; in the remaining 15 patients, probable myositis was diagnosed because of the absence of the CD8/MHC-1 complex, possibly a result of a minimal inflammatory reaction or patchy MHC-1 expression.[12–14]

In the present study, the incidence of PM was 31% (21/68), which is higher than that of other types of inflammatory myopathies. This might be

© 2011 Japanese Society for Neuroimmunology

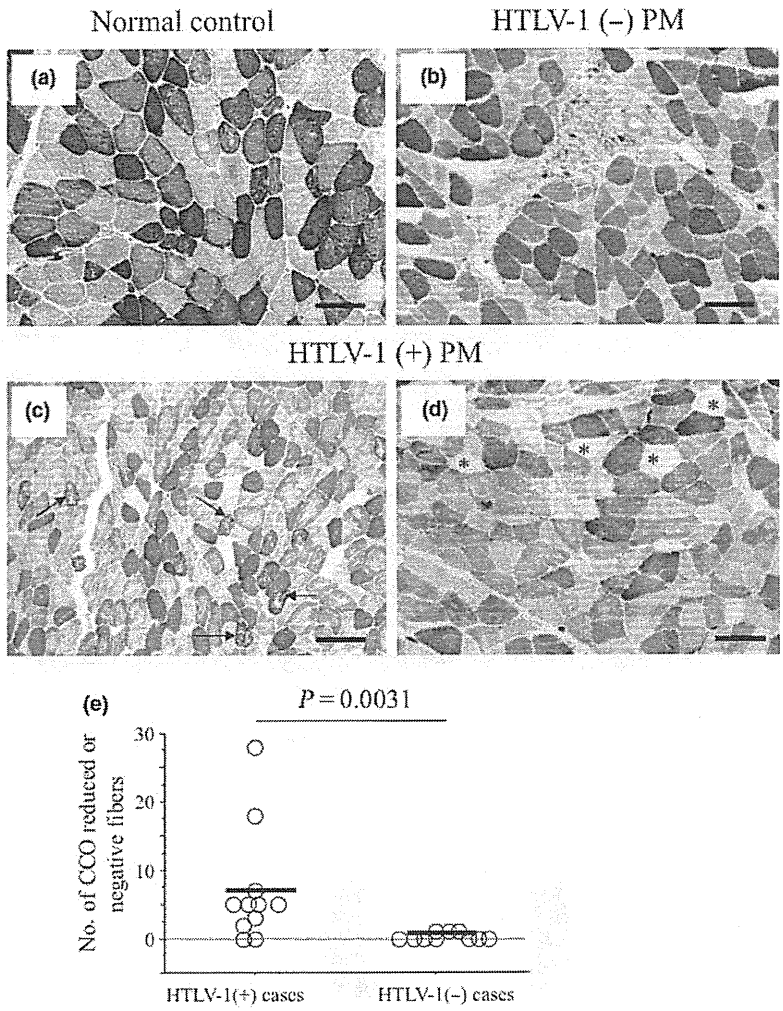

Figure 6 Enzyme histochemistry for cytochrome c oxidase (CCO). (a) Normal CCO staining in normal control showing two types of muscle fibers: type I (dark) and type II (light). (b) Normal CCO staining adjacent to inflammatory cells in human T-lymphotropic virus type 1 (HTLV-1)-negative polymyositis (PM). (c) Frequently observed partially reduced CCO-stained fibers with a mosaic appearance (arrows) in HTLV-1-positive PM. (d) Many completely CCO-negative fibers in HTLV-1-positive PM (stars). (e) Combined data for all study patients. Significantly greater numbers of partially reduced or completely CCO-negative fibers are seen in HTLV-1-positive than in HTLV-1-negative PM ($P = 0.0031$, Mann–Whitney *U*-test). Bars (a)–(d) 100 μm.

because the present study was carried out on patients with myositis in Kagoshima and Okinawa prefectures, where HTLV-1 is endemic and usually shows the PM phenotype. Therefore, the association of PM with HTLV-1 might not be coincidental. Using these 21 cases of PM, we assessed whether HTLV-1 affects the clinical course and histopathological features of myositis.[12,13]

To confirm HTLV-1 positivity, we carried out a highly sensitive nested PCR using DNA extracted from fresh frozen muscle biopsy specimens; we found that all HTLV-1-positive patients were concomitant on retrospective serological examination without any disparities. This was carried out as a confirmatory procedure to clarify the difference between HTLV-1-positive and HTLV-1-negative cases. Based on these results, we determined that there were 11 HTLV-1-seropositive and PCR positive PM cases; and 10 HTLV-1-seronegative and PCR negative PM cases.

Regarding the clinical course of the patients, we found that HTLV-1-positive PM patients show a more protracted course, because they have a significantly longer duration of illness from the onset of symptoms until the time of biopsy. The longer duration before biopsy might reflect that the disease requires more time to progress to such a degree that obligates patients to seek medical advice; at the time of biopsy, all patients had sufficient clinical and histological features for a diagnosis of myositis. Although further follow-up studies of the patients in this cohort are necessary to conclude the protracted clinical course of HTLV-1-positive PM, the results of the present study are consistent with those of previous studies carried out in Kyushu and Jamaica – both areas of endemic HTLV-1 infection[15] – that report HTLV-1-seropositive

© 2011 Japanese Society for Neuroimmunology

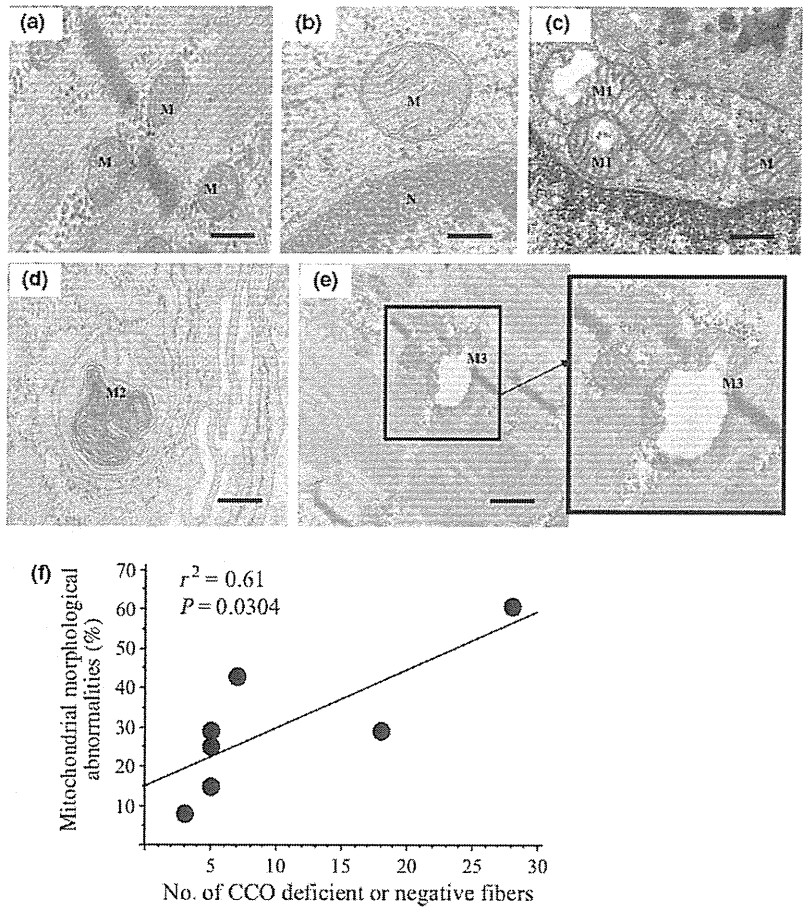

Figure 7 Ultrastructural examination of mitochondria. (a) Normal mitochondria near Z-discs in human T-lymphotropic virus type 1 (HTLV-1)-negative polymyositis (PM). (b) Normal mitochondria near the nucleus in HTLV-1-negative PM. (c) Mitochondria showing variable degrees of morphological abnormalities near the nucleus (M1) and other apparently normal mitochondria (M) in HTLV-1-positive PM. (d) Mitochondrion showing myelin-like formations in HTLV-1-positive PM (M2). (e) Well-fixed area showing many mitochondria; one of them shows abnormal high-amplitude swelling, cristae fragmentation, membrane interruption and loss of matrix in HTLV-1-positive PM (M3). (f) The percentages of mitochondria with morphological abnormalities is correlated with the counts of CCO-reduced or CCO-negative stained fibers (P = 0.0304; Spearman's rank correlation). Bars (a), (e) 0.3 μm; bars (b)–(d) 0.2 μm.

PM patients having more frequent hospital admissions and significantly longer durations of symptoms before presentation.[16–18]

At the histopathological level, although both groups showed the classical features of PM, we found the following significant features of the HTLV-1-positive PM group compared with the HTLV-1-negative PM group: (i) endomysial inflammatory infiltrates are more prominent; (ii) necrotic fibers are observed less frequently; (iii) regenerative activities are more prominent; and (iv) partial or complete CCO reduction is more frequent. The present results show significantly higher endomysial infiltration of $CD8^+$ and $CD4^+$ T-cells in HTLV-1-positive PM; some of the infiltrating $CD4^+$ cells in muscle lesions are considered to be the HTLV-1 genome-harboring cells, as we have reported in previous studies.[19,20]

We also observed the accumulation of $CD8^+$ T-cells around aberrant normal myofibers. This suggests that myositis in patients with HTLV-1 infections is not caused by direct viral infection of muscle fibers, but by an immune reaction between HTLV-1-infected $CD4^+$ cells and HTLV-1-specific $CD8^+$ cytotoxic T-cells damaging muscle fibers.[21–23] This characteristic inflammatory process associated with HTLV-1 is also detected in other tissues, such as tissues of the central nervous system in patients with HAM/TSP[24] and HTLV-1 uveitis in the eye.[25]

Regarding necrosis and regeneration, the results obtained from the present study were contrary to our expectations and were paradoxical to the general rule that regeneration follows necrosis; therefore, we preferred to designate them as regenerative processes (i.e., processes for mending or maintaining partially damaged muscle fibers) rather than regeneration. HTLV-1 was recently linked to regenerative activities via $p12^I$, which is an accessory hydrophilic protein of HTLV-1 that might contribute to and amplify the physiological stimulation of cells for proliferation.[26,27]

We speculate that such upregulation of regenerative processes contributes to the protracted course of

© 2011 Japanese Society for Neuroimmunology

Table 2 Detailed histological, histochemical and electron microscopy findings in skeletal muscle of all 21 polymyositis patients

Case	Fiber diameter (μm)	Necrotic fibers	CCO negative fibers	SDH staining profile	Rimmed vacuoles	RRF	Fiber type atrophy	Neurogenic involvement	Glycogen and lipid content	Abnormal MT (%)
Po 1	10–60	+	++	N	–	–	Both types atrophy	–	N	43
Po 2	8–50	+	–	N	–	–	Type II atrophy	–	N	NA
Po 3	10–70	+	+++	+	–	–	Type II atrophy	–	N	61
Po 4	10–70	–	+	N	–	–	Type II atrophy	–	N	NA
Po 5	10–50	+	+	N	–	–	Both types atrophy	–	N	29
Po 6	10–80	–	–	N	–	–	Both types atrophy	–	N	NA
Po 7	5–60	–	+	N	–	–	Both types atrophy	–	N	25
Po 8	8–60	+	+	N	–	–	Type II atrophy	–	N	8
Po 9	10–60	–	++	N	–	–	Both types atrophy	–	N	29
Po 10	10–60	–	+	N	–	–	Both types atrophy	–	N	15
Po 11	5–60	–	+	N	–	–	Type II atrophy	–	N	NA
Neg 1	10–50	+	+	N	–	–	Type II atrophy	–	N	–
Neg 2	8–50	+	–	N	–	–	Type II atrophy	–	N	NA
Neg 3	10–60	++	–	N	–	–	Both types atrophy	–	N	–
Neg 4	10–70	+++	–	N	–	–	Both types atrophy	–	N	NA
Neg 5	10–70	+	+	N	–	–	Both types atrophy	–	N	–
Neg 6	8–70	+	–	N	–	–	Type II atrophy	–	N	NA
Neg 7	5–60	+	–	N	–	–	Both types atrophy	–	N	–
Neg 8	10–60	++	–	+	–	–	Both types atrophy	–	N	NA
Neg 9	5–70	+	+	N	–	–	Both types atrophy	–	N	–
Neg 10	10–70	+	–	N	–	–	Both types atrophy	–	N	NA

–, Absent; +, 1–2/200 fibers, mild; ++, 3–5/200 fibers, moderate; +++, more than 5/200 fibers, frequent. Abnormal MT % is the percentage of abnormal mitochondria. CCO, cytochrome c oxidase; MT, mitochondria; N, normal; NA, not assessed; RRF, ragged red fibers; SDH, succinate dehydrogenase.

HTLV-1-positive PM. These regenerative processes might be continuous but not complete, as fibers showing such processes appear slightly smaller than others in addition to upregulation of neonatal proteins.

We observed a reduction in CCO activity in HTLV-1-positive PM with intact normal staining profiles of SDH. CCO is an enzyme that is localized in the inner membrane and cristae of mitochondria, which are multifunctional and highly complex organelles.[28] This finding attracted our attention; therefore, we examined the mitochondrial ultrastructure using electron microscopy. Mitochondrial morphological abnormalities were more frequently observed in HTLV-1-positive than in HTLV-1-negative patients or normal control subjects. Therefore, these mitochondrial morphological abnormalities are more likely to be related to HTLV-1 infection. In particular, we found a significant correlation between these morphological abnormalities and the numbers of CCO-deficient or CCO-negative fibers. Such a link between HTLV-1 and similar mitochondrial morphological abnormalities was previously observed *in vitro* and is reported to be caused by $p13^{II}$, an accessory protein of HTLV-1.[23] In addition, $p13^{II}$ accumulates in the inner mitochondrial membranes and causes mitochondrial morphological abnormalities by altering membrane permeability.[29]

It would be interesting if future studies could detect such viral proteins and confirm their relationship to the present findings *in vivo*.

In summary, we observed the clinical and morphological differences of muscle biopsy specimens between cases of HTLV-1-positive and HTLV-1-negative PM. Although these differences were significant, they were not specific to HTLV-1-positive PM, because they were also observed (although less frequently) in HTLV-1-negative PM. These results suggest that HTLV-1 is responsible for modifying the clinical course and the histopathological features of myofibers observed in the present study.

Acknowledgements

The present study was supported by a Grant-in-Aid for Scientific Research from Japan Society for the Promotion of Science and research grants from the Health Sciences Research Grants from the Ministry

© 2011 Japanese Society for Neuroimmunology

of Health, Labor, and Welfare in Japan. We thank Ms N. Hirata and Ms T. Inoue for their excellent technical assistance.

References

1. Osame M, Usuku K, Izumo S, Ijichi N, Amitani H, Igata A, et al. HTLV-I associated myelopathy, a new clinical entity. *Lancet*. 1986; **327**: 1031–2.
2. Uchiyama T. Human T cell leukemia virus type I (HTLV-I) and human diseases. *Annu Rev Immunol*. 1997; **15**: 15–37.
3. Morgan OS, Rodgers-Johnson P, Mora C, Char G. HTLV-1 and polymyositis in Jamaica. *Lancet*. 1989; **334**: 1184–7.
4. Dalakas MC. Understanding the immunopathogenesis of inclusion-body myositis: present and future prospects. *Rev Neurol*. 2002; **158**: 948–58.
5. Dalakas MC. Inflammatory, immune, and viral aspects of inclusion-body myositis. *Neurology*. 2006; **66**: 33–8.
6. Matsuura E, Umehara F, Nose H, Higuchi I, Matsuoka E, Izumi K, et al. Inclusion body myositis associated with human T-lymphotropic virus-Type I infection: eleven patients from an endemic area in Japan. *J Neuropathol Exp Neurol*. 2008; **67**: 41–9.
7. Dalakas MC, Hohlfeld R. Polymyositis and dermatomyositis. *Lancet*. 2003; **362**: 971–82.
8. Dalakas MC. Polymyositis, dermatomyositis and inclusion body myositis. *N Engl J Med*. 1991; **325**: 1487–98.
9. Dubowitz V, Brooke MH. The procedure of muscle biopsy. Muscle Biopsy: A Modern Approach. Dubowitz V, Brooke MH, Neville HE, eds. London, Philadelphia, Toronto: WB Saunders; 1973: 5–102.
10. Kubota R, Fujiyoshi T, Izumo S, Yashiki S, Maruyama I, Osame M, et al. Fluctuation of HTLV-I proviral DNA in peripheral blood mononuclear cells of HTLV-I-associated myelopathy. *J Neuroimmunol*. 1993; **42**: 147–54.
11. Nagai M, Usuku K, Matsumoto W, Kodama D, Takenouchi N, Moritoyo T, et al. Analysis of HTLV-I proviral load in 202 HAM/TSP patients and 243 asymptomatic HTLV-I carriers: high proviral load strongly predisposes to HAM/TSP. *J Neurovirol*. 1998; **4**: 586–93.
12. Amato AA, Griggs RC. Unicorns, dragons, polymyositis, and other mythological beasts. *Neurology*. 2003; **61**: 288–90.
13. Van der Meulen MF, Bronner IM, Hoogendijk JE, Burger H, Van Venrooij WJ, Voskuyl AE, et al. Polymyositis: an overdiagnosed entity. *Neurology*. 2003; **6**: 316–21.
14. Dalakas MC. Inflammatory disorders of muscle: progress in polymyositis, dermatomyositis and inclusion body myositis. *Curr Opin Neurol*. 2004; **17**: 561–7.
15. Gessain A. Epidemiology of HTLV-1 and associated diseases. Human T-cell Lymphotropic Virus Type-1. Höllsberg P, Hafler DA, eds. Chiester: Wiley; 1997: 33–64.
16. Higuchi I, Nerenberg M, Yoshimine K, Yoshida M, Fukunaga H, Tajima K, et al. Failure to detect HTLV-I by in situ hybridization in the biopsied muscles of viral carriers with polymyositis. *Muscle Nerve*. 1992; **15**: 43–7.
17. Higuchi I, Hashimoto K, Kashio N, Izumo S, Inose M, Izumi K, et al. Detection of HTLV-I provirus by in situ polymerase chain reaction in mononuclear inflammatory cells in skeletal muscle of viral carriers with polymyositis. *Muscle Nerve*. 1995; **18**: 854–8.
18. Gilbert DT, Morgan O, Smikle MF, Simeon D, Barton EN. HTLV-1 associated polymyositis in Jamaica. *Acta Neurol Scand*. 2001; **104**: 101–4.
19. Higuchi I, Hashimoto K, Matsuoka E, Rosales R, Nakagawa M, Arimura K, et al. The main HTLV-I-harboring cells in the muscles of viral carriers with polymyositis are not macrophages but CD4+ lymphocytes. *Acta Neuropathol*. 1996; **92**: 358–61.
20. Saito M, Higuchi I, Saito A, Izumo S, Usuku K, Bangham CR, et al. Molecular analysis of T cell clonotypes in muscle-infiltrating lymphocytes from patients with human T lymphotropic virus type 1 polymyositis. *J Infect Dis*. 2002; **186**: 1231–41.
21. Ozden S, Gessain A, Gout O, Mikol J. Sporadic inclusion body myositis in a patient with human T cell leukemia virus type 1-associated myelopathy. *Clin Infect Dis*. 2001; **32**: 510–4.
22. Ozden S, Cochet M, Mikol J, Teixeira A, Gessain A, Pique C. Direct evidence for a chronic CD8+-T-cell-mediated immune reaction to tax within the muscle of a human T-cell leukemia/lymphoma virus type 1-infected patient with sporadic inclusion body myositis. *J Virol*. 2004; **78**: 10320–7.
23. Kohsaka H. Current insights in polymyositis and dermatomyositis. *Clin and Exp Neuroimmunol*. 2010; **1**: 22–32.
24. Umehara F, Izumo S, Nakagawa M, Ronquillo AT, Takahashi K, Matsumuro K, et al. Immunocytochemical analysis of the cellular infiltrate in the spinal cord lesions in HTLV-I-associated myelopathy. *J Neuropathol Exp Neurol*. 1993; **52**: 424–30.
25. Mochizuki M. Regional immunity of the eye. *Acta Ophthalmol*. 2010; **88**: 292–9.
26. Ciminale V, Zotti L, D'Agostino DM, Ferro T, Casareto L, Franchini G, et al. Mitochondrial targeting of the p13II protein coded by the x-II ORF of human T-cell leukemia/lymphotropic virus type I (HTLV-I). *Oncogene*. 1999; **18**: 4505–14.
27. Nicot C, Harrod RL, Ciminale V, Franchini G. Human T-cell leukemia/lymphoma virus type 1 nonstructural genes and their functions. *Oncogene*. 2005; **24**: 6026–34.
28. Chariot P, Monnet I, Gherardi R. Cytochrome C oxidase reaction improves histopathological assessment of zidovudine myopathy. *Ann Neurol*. 1993; **34**: 561–5.
29. D'Agostino DM, Ranzato L, Arrigoni G, Cavallari I, Belleudi F, Torrisi MR, et al. Mitochondrial alterations induced by the $p13^{II}$ protein of human T-cell leukemia virus type 1. Critical role of arginine residues. *J Biol Chem*. 2002; **277**: 34424–33.

© 2011 Japanese Society for Neuroimmunology

MAJOR ARTICLE

Reduced Tim-3 Expression on Human T-lymphotropic Virus Type I (HTLV-I) Tax-specific Cytotoxic T Lymphocytes in HTLV-I Infection

Nashwa H. Abdelbary,[1] Hazem M. Abdullah,[1] Toshio Matsuzaki,[2] Daisuke Hayashi,[2] Yuetsu Tanaka,[3] Hiroshi Takashima,[2] Shuji Izumo,[1] and Ryuji Kubota[1]

[1]Division of Molecular Pathology, Center for Chronic Viral Diseases and [2]Department of Neurology and Geriatrics, Graduate School of Medical and Dental Sciences, Kagoshima University, 8-35-1 Sakuragaoka, Kagoshima, Japan; and [3]Department of Immunology, Graduate School and Faculty of Medicine, University of the Ryukyus, Uehara 207, Nishihara-cho, Okinawa, Japan

T cell immunoglobulin and mucin domain-containing molecule-3 (Tim-3) and programmed cell death-1 (PD-1) are T cell exhaustion molecules. We investigated the expression of Tim-3 and PD-1 in human T-lymphotropic virus type I (HTLV-I) infection. Tim-3 expression, but not PD-1 expression, was reduced on $CD4^+$ and $CD8^+$ T cells of HTLV-I–associated myelopathy/tropical spastic paraparesis (HAM/TSP) patients and HTLV-I carriers as compared with healthy controls. Tim-3 expression was also reduced in HTLV-I Tax-specific cytotoxic T lymphocytes (CTLs) as compared with cytomegalovirus-specific CTLs. Tim-3^+, but not PD-1^+, Tax-specific CTLs produced less interferon-γ and exhibited low cytolytic activity. However, we observed no difference in the expression of Tim-3 or cytolytic activity between Tax-specific CTLs of HAM/TSP patients or carriers. Moreover, HTLV-I–infected $CD4^+$ T cells showed decreased Tim-3 expression. These data suggest that Tim-3 expression is reduced in HTLV-I infection and that a high number of Tim-3^- HTLV-I–specific CTLs preserves their cytolytic activity, thereby controlling viral replication.

INTRODUCTION

Human T-lymphotropic virus type I (HTLV-I) is a retrovirus that preferentially infects $CD4^+$ lymphocytes in vivo [1]. Although HTLV-I infection is lifelong, less than 1% of infected individuals develop HTLV-I–associated myelopathy/tropical spastic paraparesis (HAM/TSP), a neurologic disease, or adult T cell leukemia (ATL), a hematologic disease [2–4]. HAM/TSP is an inflammatory disease of the spinal cord characterized by infiltration of inflammatory cells into the perivascular area [5]. Patients with HAM/TSP show spastic paraparesis and sphincter dysfunction with mild sensory disturbance [6]. HTLV-I proviral load and frequency of HTLV-I–specific $CD8^+$ cytotoxic T lymphocytes (CTLs) are higher in the peripheral blood of patients with HAM/TSP as compared with asymptomatic carriers [7–9]. Although increasing evidence supports the hypothesis that such a strong CTL response could certainly contribute to the control of viral replication and disease development, the exact pathogenic role of the CTL responses remains unclear [10].

The T-cell receptor costimulatory pathways assist in regulating T cell activation or tolerance [11, 12]. Recently, programmed cell death-1 (PD-1) signaling was shown to play an important role in T cell exhaustion during chronic viral infections [13–16]. T cell immunoglobulin and mucin domain-containing molecule-3 (Tim-3) has been similarly associated with T cell exhaustion [17]. Interaction of Tim-3 with its ligand galectin-9 regulates Th1 cell responses by promoting the

Received 13 July 2010; accepted 15 November 2010.
Potential conflicts of interest: none reported.
Reprints or correspondence: Ryuji Kubota, MD, Division of Molecular Pathology, Center for Chronic Viral Diseases, Graduate School of Medical and Dental Sciences, Kagoshima University, 8-35-1 Sakuragaoka, Kagoshima 890-8544, Japan (E-mail: kubotar@m2.kufm.kagoshima-u.ac.jp).

The Journal of Infectious Diseases 2011;203:948–59
© The Author 2011. Published by Oxford University Press on behalf of the Infectious Diseases Society of America. All rights reserved. For Permissions, please e-mail: journals.permissions@oup.com
1537-6613/2011/2037-0001$15.00
DOI: 10.1093/infdis/jiq153

Downloaded from http://jid.oxfordjournals.org/ at Kagoshima University on April 10, 2012

death of interferon-γ (IFN-γ)–producing Th1 cells [18]. A recent study of human immunodeficiency virus (HIV) and hepatitis C virus (HCV) infections demonstrated that Tim-3 is upregulated in $CD4^+$ and $CD8^+$ T cells of patients with chronic viral infection. Tim-3-expressing T cells secrete less IFN-γ than do Tim-3-negative cells [19, 20]. In addition, a reduction of Tim-3 expression in T cells by using small interfering RNA or blocking antibodies increases the secretion of the antiviral cytokine IFN-γ [20, 21]. However, it is unclear whether T cells are exhausted or Tim-3 expression is upregulated in HTLV-I infection.

It remains unknown why only a small number of HTLV-I–infected individuals develop HAM/TSP, while the majority of the infected persons remain disease-free. It has been clearly demonstrated that elevated HTLV-I proviral loads increase the risk of HAM/TSP development [7, 22]. In addition, HAM/TSP patients have more HTLV-I–specific CTLs than do asymptomatic carriers [8, 23]. Recently, it has been postulated that CTLs in HAM/TSP patients have impaired function in association with degranulation of cytolytic molecules as compared with CTLs in asymptomatic carriers, which may result in an insufficient control of the virus [24]. However, it remains unclear whether CTL function is impaired in HAM/TSP patients.

In this study, we investigated Tim-3 and PD-1 expression in HTLV-I infection. In particular, we studied HTLV-I–specific CTLs and their degranulation activity in HAM/TSP patients and asymptomatic carriers as well as the role of Tim-3 and PD-1 in regulating their function.

MATERIALS AND METHODS

Patients

The study subjects consisted of 32 HAM/TSP patients, 31 asymptomatic carriers, and 11 uninfected healthy controls (Table 1). All subjects were residents of Kagoshima Prefecture, Japan. HTLV-I infection was determined using a HTLV-I antibody serological test, and HAM/TSP was diagnosed according to World Health Organization guidelines. All patients gave their written informed consent to participate in this study. Peripheral blood mononuclear cells (PBMCs) were separated from heparinized blood by Ficoll gradient centrifugation and stored in liquid nitrogen until use. To investigate HTLV-I–specific CTLs, we selected HLA-A*0201-positive or HLA-A*2402-positive cases because HTLV-I Tax11–19 and Tax301–309 are well characterized and strong immunodominant epitopes are restricted to these HLAs [25–27]. This study was reviewed and approved by the Kagoshima University Ethical Committee.

Cell Surface Staining

After thawing, 1×10^6 PBMCs were stained with a rat IgG2a anti-Tim-3 antibody (R&D Systems). The cells were washed with a staining buffer (PBS containing 5% normal goat serum and 0.1% NaN_3) and further stained with a goat anti-rat IgG–Alexa Fluor 488 secondary antibody (Invitrogen). Alternatively, the cells were stained with an anti-PD-1–fluorescein isothiocyanate (FITC) (eBioscience), anti-CD3–energy-coupled dye (ECD), anti-CD4–phycoerythrin (PE)–Cy5 (PC5), or anti-CD8–PC5 antibody (Beckman Coulter), and a PE-labeled tetramer. The HLA/antigen tetramers used were as follows: HLA-A*0201/HTLV-I Tax11–19 (LLFGYPVYV), HLA-A*0201/CMV pp65 (NLVPMVATV), HLA-A*0201/HIV Gag (SLYNTVATL), HLA-A*2402/HTLV-I Tax301–309 (SFHSLHLLF), HLA-A*2402/CMV pp65 (QYDPVAALF), and HLA-A*2402/HIV Gag (RYLKDQQLL) (Medical & Biological Laboratories). Alternatively, the cells were stained with anti-PD-L1–PE (eBioscience), anti-CD3–ECD, CD4–PC5 and CD8–FITC antibody (Beckman Coulter). Appropriate isotype antibodies were used as controls. Fluorescent signal was detected by an Epics XL flow cytometer, and Expo32 software was used for data acquisition and analysis (Beckman Coulter).

Intracellular IFN-γ Detection

PBMCs were cultured in complete medium (RPMI 1640 medium supplemented with 100 U/mL penicillin, 0.1 mg/mL streptomycin, and 10% heat-inactivated fetal cow serum) in the absence or presence of phorbol 12-myristate 13-acetate (PMA [5 ng/mL]) and ionomycin (0.5 μg/mL) with 5 μg/mL of the secretion inhibitor brefeldin A (Sigma) for 6 hours. After harvesting, the cells were stained with a rat anti-Tim-3 antibody, followed by staining with a goat anti-rat IgG–PC5 secondary antibody (Santa Cruz Biotechnology), or with an anti-PD-1–FITC antibody. The cells were then stained with an anti-CD8–ECD antibody (Beckman Coulter) and Tax tetramer–PE. The cells were fixed with 1% paraformaldehyde, resuspended in 50 μL permeabilization buffer (0.1% saponin in staining buffer),

Table 1. Clinical Characteristics of the Study Groups

Subject	Number	Age (mean [SD])	Sex (M/F)[a]	HTLV-I proviral load[b] mean (SD)
HAM/TSP[c]	32	34–73 (57.8 [10.8])	11/21	2091.6 (3606.9)
Asymptomatic carrier	31	22–78 (55.3 [11.6])	10/21	608.9 (1159.9)
Healthy control	11	36–66 (49.4 [9.7])	1/10	N/A[d]

NOTE. [a] M/F: male/female.
[b] copies/10^4 cells.
[c] HAM/TSP: HTLV-I–associated myelopathy/tropical spastic paraparesis.
[d] N/A: not applicable.

Downloaded from http://jid.oxfordjournals.org/ at Kagoshima University on April 10, 2012

and stained with an anti-IFN-γ–FITC antibody (Immunotech). For PD-1 detection, the cells were stained with anti-IFN-γ–biotin (eBioscience) followed by staining with a streptavidin–PC5 secondary antibody (Becton Dickinson). At least 3×10^5 $CD8^+$ cells were examined by flow cytometry.

CD107a Degranulation Assay

Cytolytic activity was assessed by flow cytometric quantification of the surface mobilization of CD107a (cluster of differentiation 107a, an integral membrane protein in cytolytic granules) [28]. PBMCs (1×10^6) from patients with HLA-A*02 were pulsed with 1 μM HTLV-I Tax11–19 or with the control influenza virus M1 peptide (GILGFVFTL) for 30 minutes; PBMCs from HLA-A*24 patients were pulsed with 1 μM HTLV-I Tax301–309 or with HIV Gag (RYLKDQQLL) peptide. Excess peptides were washed out and the cells were incubated with an anti-CD107a–PC5 antibody (Becton Dickinson [4 μL/mL]) in the presence of brefeldin A (5 μg/mL) for 4 hours. After harvesting, the cells were stained with a rat anti-Tim-3 antibody followed by an anti-rat IgG–Alexa Fluor 488 secondary antibody, or with an anti-PD-1–FITC antibody followed by staining with Tax tetramer–PE and an anti-CD8–ECD antibody. At least 1×10^5 $CD8^+$ T cells were examined by flow cytometry.

Quantitative Polymerase Chain Reaction of the HTLV-I Proviral Load

Genomic DNA was extracted from PBMCs by using the Qiagen DNA extraction kit (Qiagen). The measurements were performed as described elsewhere [7].

Intracellular HTLV-I Tax Staining

PBMCs (5×10^5) were cultured for 12 hours in complete medium in the presence of brefeldin A. After harvesting, the cells were stained with an anti-Tim-3 antibody followed by an Alexa Fluor 488-labeled secondary antibody, or with an anti-PD-1–FITC antibody and then stained with an anti-CD4–PC5 or anti-CD8–PC5 antibody. The cells were intracellularly stained with a mouse IgG3 anti-HTLV-I Tax antibody (clone Lt-4) [29] followed by a goat anti-mouse IgG3–PE antibody (Southern Biotech).

Statistical Analysis

Mann–Whitney *U* test, Wilcoxon signed-rank test, and Spearman's rank correlation test were performed using StatView software version 5.0 (SAS Institute). *P* values of less than .05 were considered significant.

RESULTS

Low Frequency of Tim-3^+ Cells Within $CD4^+$ and $CD8^+$ T cell Populations in HTLV-I Infection

Tim-3^+ cells within the lymphocyte gate were greatly reduced in asymptomatic carriers and HAM/TSP patients as compared with healthy controls (Figure 1*A*, upper row). We observed reduced frequencies of Tim-3-expressing $CD3^+CD4^+$ T cells in HTLV-I-infected individuals (mean [SD]: 2.59% [1.3%] for asymptomatic carriers and 2.62% [1.3%] for HAM/TSP patients) compared with those in healthy controls (3.72% [1.5%]) ($P = .031$ and $P = .034$, respectively [Figure 1*B*]). The same was observed on $CD3^+CD8^+$ T cells of infected individuals (7.19% [4.3%] for asymptomatic carriers and 7.54% [4.4%] for HAM/TSP patients) compared with those in healthy controls (10.6% [3.2%]) ($P = .026$ and $P = .021$, respectively [Figure 1*B*]). However, we observed increased mean fluorescent intensity (MFI) of Tim-3-expressing $CD4^+$ and $CD8^+$ T cells in asymptomatic carriers as compared with healthy controls ($P = .0031$ and $P = .046$, respectively [Figure 1*C*]). Conversely, we could not detect significant differences in Tim-3 expression (neither frequency nor MFI) on $CD4^+$ or $CD8^+$ T cells of HAM/TSP patients and asymptomatic carriers (Figures 1*B* and 1*C*). The frequency of Tim-3^+ cells within $CD4^+$ or $CD8^+$ T cells did not correlate with HTLV-I proviral loads in HAM/TSP patients, asymptomatic carriers, or when both groups were combined (data not shown).

Low Expression of Tim-3 on HTLV-I Tax-specific CTLs as compared With That on Cytomegalovirus-specific CTLs in HTLV-I Infection

Tim-3 expression on antigen-specific $CD8^+$ T cells was examined in 9 HLA-A*02 HAM/TSP patients using HLA/antigen tetramers, as shown in Figure 2*A*. We found significantly lower levels of Tim-3 on HTLV-I Tax-specific versus cytomegalovirus (CMV)–specific CTLs in HAM/TSP patients ($P = .038$ [Figure 2*B*]). The frequency of Tim-3–expressing Tax-specific CTLs was significantly lower than that in the total $CD8^+$ T-cell population ($P = .0077$ [Figure 2*B*]). The frequencies of Tax-specific CTLs in HLA-A^*02^+ asymptomatic carriers were too low to reliably evaluate Tim-3 expression on these cells. Using PBMCs from 9 HAM/TSP patients and 10 asymptomatic carriers with HLA-A*24, we found that the frequency of Tim-3–expressing Tax-specific CTLs was also significantly lower than that in the total $CD8^+$ T cell population ($P = .0077$ and $P = .013$, respectively [Figures 2*C* and 2*D*]). We attempted to assess Tim-3 expression on CMV $tetramer^+$ cells in this HLA-A*24 group but the frequencies of CMV-specific CTLs were too small to reliably evaluate Tim-3 expression. As expected, the frequency of Tax-specific CTLs was higher in HAM/TSP patients than in asymptomatic carriers (Figure 2*E*). The frequency of Tim-3^+ cells in Tax-specific CTLs was not different between the 2 groups (Figure 2*F*). However, the MFI of Tim-3 in Tax-specific CTLs was significantly higher in asymptomatic carriers than in HAM/TSP patients ($P = .0084$ [Figure 2*G*]). In addition, we detected no correlation between the frequency of Tim-3^+ Tax-specific CTLs and HTLV-I proviral load, duration of illness, disease

Downloaded from http://jid.oxfordjournals.org/ at Kagoshima University on April 10, 2012

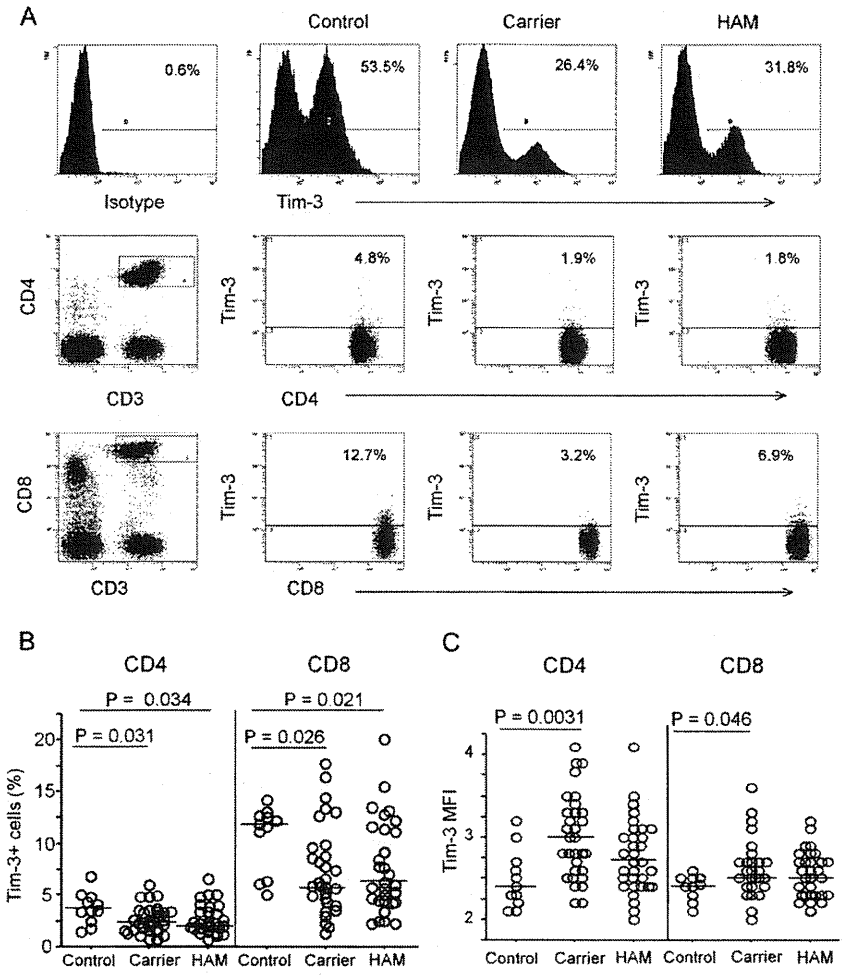

Figure 1. Low frequency of Tim-3$^+$ cells within the CD4$^+$ and CD8$^+$ T cell populations in HTLV-I infection. PBMCs from 63 HTLV-I–infected (32 HAM/TSP patients and 31 carriers) and 11 uninfected subjects were stained with antibodies against CD3, CD4, or CD8 and Tim-3. The numbers indicate the percentage of Tim-3$^+$ cells within each cell population. (*A*) Representative data from each group are shown in the last 3 columns. The upper row shows the expression levels of Tim-3 in total lymphocytes. The middle and lower rows show Tim-3 expression in CD3$^+$CD4$^+$ and CD3$^+$CD8$^+$ cells, respectively. (*B*) The combined data from all studied subjects reveal significantly lower percentages of Tim-3$^+$ cells within CD4$^+$ and CD8$^+$ T cell populations of HAM/TSP patients and carriers than those of controls. Each symbol represents an individual subject, and the horizontal bars indicate the medians. Data were analyzed by Mann–Whitney *U* test. (*C*) The combined data from all studied subjects reveal significantly higher MFI of Tim-3$^+$ cells in CD4$^+$ and CD8$^+$ T cell populations of carriers than those of controls. Data were analyzed by Mann–Whitney *U* test. Each symbol represents an individual subject, and the horizontal bars indicate the medians in each group.

NOTE: PBMCs: peripheral blood mononuclear cells; HAM/TSP: HTLV-I–associated myelopathy/tropical spastic paraparesis; Tim-3: T cell immunoglobulin and mucin domain-containing molecule-3; MFI: mean fluorescent intensity; HAM: HTLV-I–associated myelopathy/tropical spastic paraparesis.

activity, age of the patients, or serum HTLV-1 antibody titer (data not shown).

Increased PD-1 Expression on HTLV-I Tax-specific CTLs as Compared With That on CMV-specific CTLs

Since PD-1 has been also recognized as a marker for T cell exhaustion, we assessed PD-1 expression levels in 9 HAM/TSP patients, 8 asymptomatic carriers, and 10 healthy controls (Figure 3*A*). We could not detect a significant difference in PD-1 expression (neither frequency nor MFI) between HAM/TSP patients, asymptomatic carriers, and healthy controls in either CD4$^+$ or CD8$^+$ T cells (Figure 3*B*). However, we observed a significantly higher frequency of PD-1–expressing Tax-specific CTLs in asymptomatic carriers as compared with that in HAM/TSP patients (P = .043 [Figure 3*C*]). We assessed PD-L1 expression levels in all three groups. Since expression levels were relatively small (0.07–0.76%) in either CD3$^+$CD4$^+$ or CD3$^+$CD8$^+$ cells, we did not consider these results. Next, we analyzed PD-1 expression on antigen-specific cells (Figure 3*D*) and found significantly higher PD-1 expression on Tax-specific CTLs as compared with CMV-specific CTLs (P = .046

Downloaded from http://jid.oxfordjournals.org/ at Kagoshima University on April 10, 2012

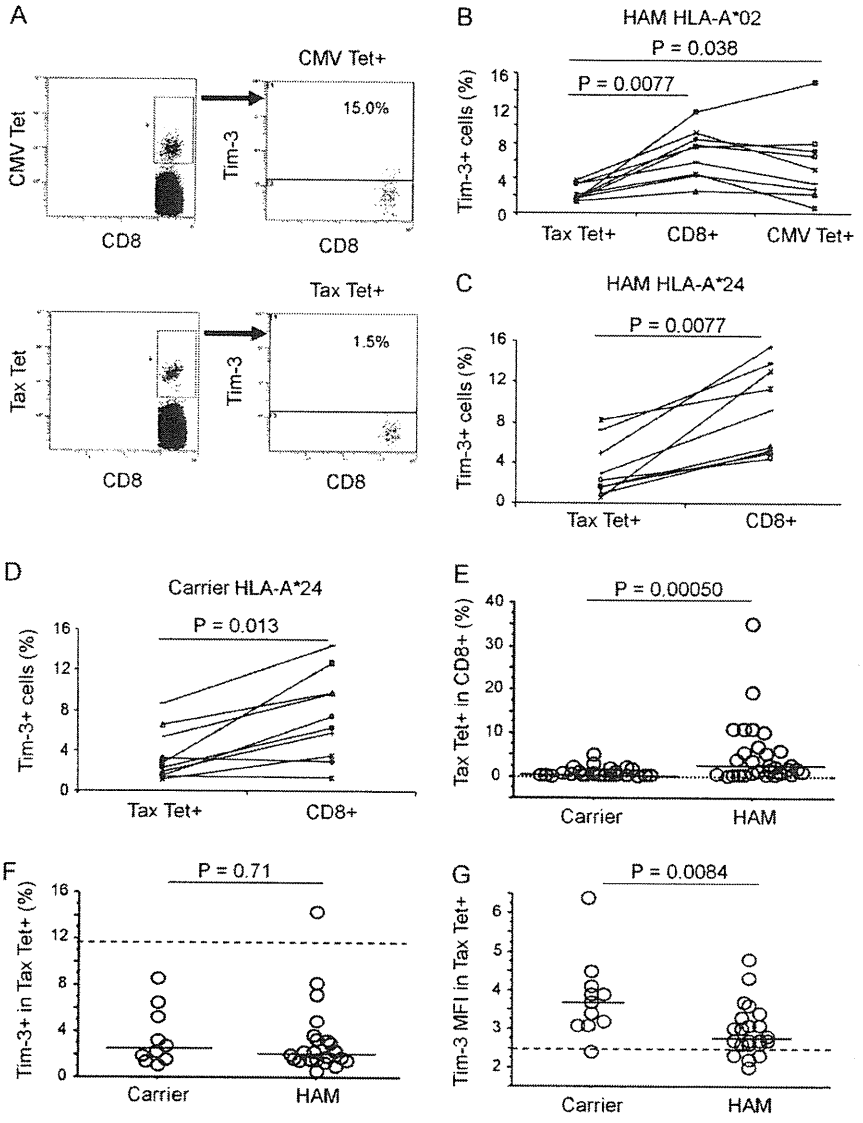

Figure 2. Low expression of Tim-3 on HTLV-I Tax-specific CTLs as compared with that on CMV-specific CTLs in HTLV-I infection. Tim-3 expression was determined in $CD8^+$, $CD8^+$Tax $tetramer^+$, and $CD8^+$CMV $tetramer^+$ cells of HAM/TSP patients and carriers. (*A*) A representative flow cytometry analysis depicts Tim-3 expression on $tetramer^+$ cells from a HAM/TSP patient. Gated $CD8^+tetramer^+$ cells were used for quantification of Tim-3^+ cells. The upper and bottom rows show Tim-3 expression in CMV-specific and HTLV-I Tax-specific CTLs. The numbers indicate the percentage of Tim-3^+ cells in each of the $tetramer^+$ cell populations. (*B*) The combined data from 9 HLA-A*02^+ HAM/TSP patients show significantly lower expression of Tim-3 in Tax-specific CTLs than in total $CD8^+$ T cells or CMV-specific CTLs, by Wilcoxon signed-rank test. (*C, D*) The combined data from 9 HAM/TSP patients and 10 carriers, all HLA-A*24^+, show significantly lower expression of Tim-3 in Tax-specific CTLs in comparison to total $CD8^+$ T cells, by Wilcoxon signed-rank test. (*E*) The percentage of Tax $tetramer^+$ cells within the $CD8^+$ cell population in HAM/TSP patients and carriers is depicted. Patients have significantly higher number of Tax $tetramer^+$ cells as compared with carriers, by Mann–Whitney *U* test. (*F, G*) Tim-3^+ cells in $CD8^+$Tax $tetramer^+$ cells of HAM/TSP patients and carriers are shown. There is no significant difference in the frequency of Tim-3^+ cells between the 2 groups. The carriers show significantly higher MFI of Tim-3 than do HAM/TSP patients. Data were analyzed by Mann–Whitney *U* test.

NOTE: In *E–G*, each symbol represents an individual subject and the horizontal bars indicate the medians in each group. In *F* and *G*, the dashed lines indicate the medians of Tim-3^+ cells within the $CD8^+$ cell population from healthy controls. Tim-3: T cell immunoglobulin and mucin domain-containing molecule-3; HAM/TSP: HTLV-I–associated myelopathy/tropical spastic paraparesis; CMV: cytomegalovirus; HTLV-I: human T-lymphotropic virus type I; CTLs: cytotoxic T lymphocytes; MFI: mean fluorescent intensity; HAM: HTLV-I–associated myelopathy/tropical spastic paraparesis; Tet: tetramer.

Downloaded from http://jid.oxfordjournals.org/ at Kagoshima University on April 10, 2012

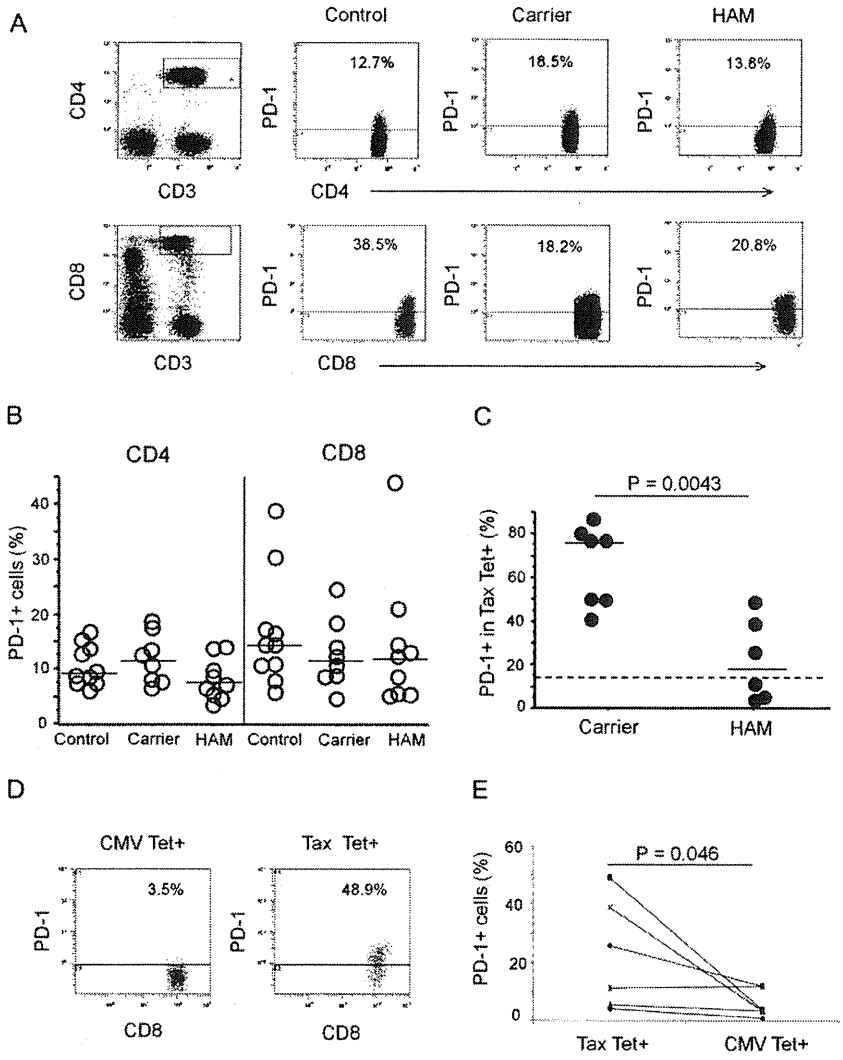

Figure 3. Increased PD-1 expression on HTLV-I Tax-specific CTLs as compared with that on CMV-specific CTLs. PD-1 expression was analyzed in PBMCs from 9 HAM/TSP patients, 8 carriers, and 10 controls after gating $CD3^+CD4^+$, $CD3^+CD8^+$, $CD8^+$Tax tetramer$^+$, or $CD8^+$CMV tetramer$^+$ cells. (*A*) The left column shows gated $CD3^+CD4^+$ and $CD3^+CD8^+$ cells. The last 3 columns show representative data of PD-1 expression in a control, a carrier, and a HAM/TSP patient after gating. (*B*) The combined data from all studied subjects show no significant difference in PD-1 expression between the 3 groups in $CD4^+$ or $CD8^+$ T cells, by Mann–Whitney *U* test. (*C*) The frequencies of PD-1^+ cells within $CD8^+$Tax tetramer$^+$ cells in HAM/TSP patients and carriers are shown. The carriers show significantly higher frequencies than HAM/TSP patients, by Mann–Whitney *U* test. The bars indicate the medians. The dashed line indicates the median value of PD-1^+ cells within the $CD8^+$ cell population from healthy controls. (*D*) The plots depict representative PD-1 expression in either $CD8^+$CMV tetramer$^+$ or $CD8^+$Tax tetramer$^+$ cells. Tax tetramer$^+$ cells show higher PD-1 expression than CMV tetramer$^+$ cells. (*E*) The combined data from 6 HAM/TSP patients show significantly higher expression of PD-1 in Tax tetramer$^+$ cells than in CMV tetramer$^+$ cells, by Wilcoxon signed-rank test.

NOTE: PD-1: programmed cell death-1; PBMCs: peripheral blood mononuclear cells; HAM/TSP: HTLV-I–associated myelopathy/tropical spastic paraparesis; CMV: cytomegalovirus; HAM: HTLV-I–associated myelopathy/tropical spastic paraparesis; Tet: tetramer.

[Figure 3*E*]). We detected no correlation between the frequency of PD-1^+ Tax-specific CTLs and HTLV-I proviral load, duration of illness, disease activity, age of the patients, or serum HTLV-1 antibody titer (data not shown). For technical reasons, we could not establish a double staining protocol for Tim-3 and PD-1.

Reduced IFN-γ Production by Tim-3^+ HTLV-I Tax-specific CTLs

We compared IFN-γ production after PMA/ionomycin stimulation between Tim-3^+ and Tim-3^- cells, or PD-1^+ and PD-1^- cells, within $CD8^+$ or Tax-specific CTL populations. As shown in Figures 4*A* and 4*D*, we determined the percentage of IFN-γ^+ cells after gating on either $CD8^+$ or $CD8^+$Tax tetramer$^+$ cells from HAM/TSP patients with a high percentage of tetramer$^+$ cells. IFN-γ was predominately produced by Tim-3^- cells, and less by Tim-3^+ cells in both groups (Figures 4*B* and 4*C*). Statistical analysis showed a significant difference in IFN-γ production (frequency and MFI) within $CD8^+$ cells (P = .043 and .043,

Downloaded from http://jid.oxfordjournals.org/ at Kagoshima University on April 10, 2012

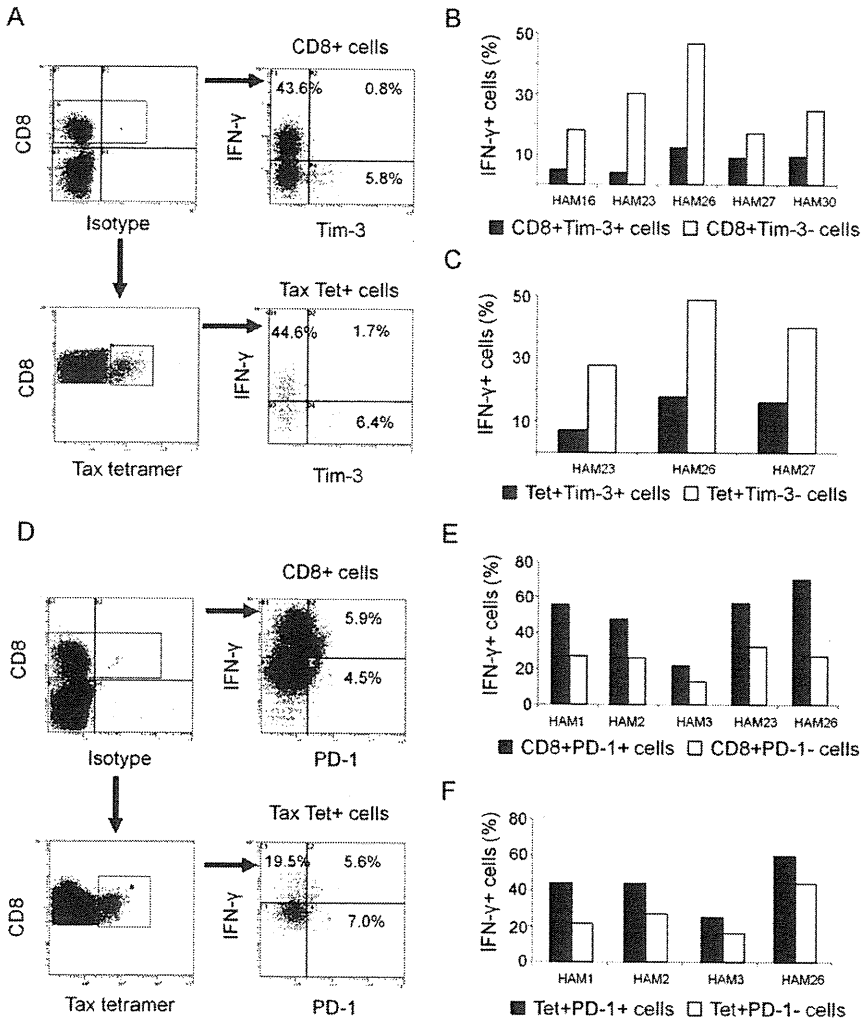

Figure 4. Reduced IFN-γ production by Tim-3$^+$ HTLV-I Tax-specific CTLs. PBMCs from 5 HAM/TSP patients were stimulated with PMA and ionomycin, and cultured for 6 hours in the presence of brefeldin A. IFN-γ production was determined by flow cytometry in CD8$^+$ and CD8$^+$Tax tetramer$^+$ cells with or without Tim-3 or PD-1 expression. (*A, D*) Representative data from a HAM/TSP patient are shown. The upper and lower rows show the percentage of IFN-γ$^+$ cells in gated CD8$^+$ and CD8$^+$Tax tetramer$^+$ cell populations, respectively. In *A*, Tim-3$^+$ cells within CD8$^+$ and Tax tetramer$^+$ cell populations have a lower percentage of INF-γ$^+$ cells than do Tim-3$^-$ cells. In *D*, PD-1$^+$ cells within CD8$^+$ and Tax tetramer$^+$ cell populations have a higher percentage of INF-γ$^+$ cells than do PD-1$^-$ cells. (*B*) Summary data from 5 HAM/TSP patients show a significantly lower percentage of INF-γ$^+$ cells within the CD8$^+$Tim-3$^+$ cell population than within the CD8$^+$Tim-3$^-$ one, after background subtraction ($P = .043$ by Wilcoxon signed-rank test). (*C*) Summary data from 3 HAM/TSP patients with high percentage of CTLs show a lower percentage of INF-γ$^+$ cells within the Tax tetramer$^+$Tim-3$^+$ cell population than within the Tax tetramer$^+$Tim-3$^-$ one, after background subtraction. (*E*) Summary data from 5 HAM/TSP patients show a significantly higher percentage of INF-γ$^+$ cells within the CD8$^+$PD-1$^+$ cell population than within the CD8$^+$PD-1$^-$ one ($P = .043$ by Wilcoxon signed-rank test). (*F*) Summary data from 4 HAM/TSP patients with high percentage of CTLs show a higher percentage of INF-γ$^+$ cells within the Tax tetramer$^+$PD-1$^+$ cell population than within the Tax tetramer$^+$ PD-1$^-$ one.

NOTE: PBMCs: peripheral blood mononuclear cells; HAM/TSP: HTLV-I–associated myelopathy/tropical spastic paraparesis; PMA: phorbol 12-myristate 13-acetate; INF-γ: interferon-γ; Tim-3: T cell immunoglobulin and mucin domain-containing molecule-3; PD-1: programmed cell death-1; CTLs: cytotoxic T lymphocytes; Tet: tetramer.

respectively). Conversely, IFN-γ was predominately produced by PD-1$^+$ cells and less by PD-1$^-$ cells in both groups (Figures 4*E* and 4*F*). Statistical analysis showed a significant difference in IFN-γ production within CD8$^+$ cells, as measured by frequency ($P = .043$). However, no difference was observed in the MFI.

Reduced CD107a Expression on Tim-3$^+$ HTLV-I Tax-specific CTLs

To assess the cytolytic activity of HTLV-I Tax-specific CTLs with or without Tim-3 or PD-1 expression, we measured CD107a expression after specific peptide stimulation of Tax-specific

Downloaded from http://jid.oxfordjournals.org/ at Kagoshima University on April 10, 2012

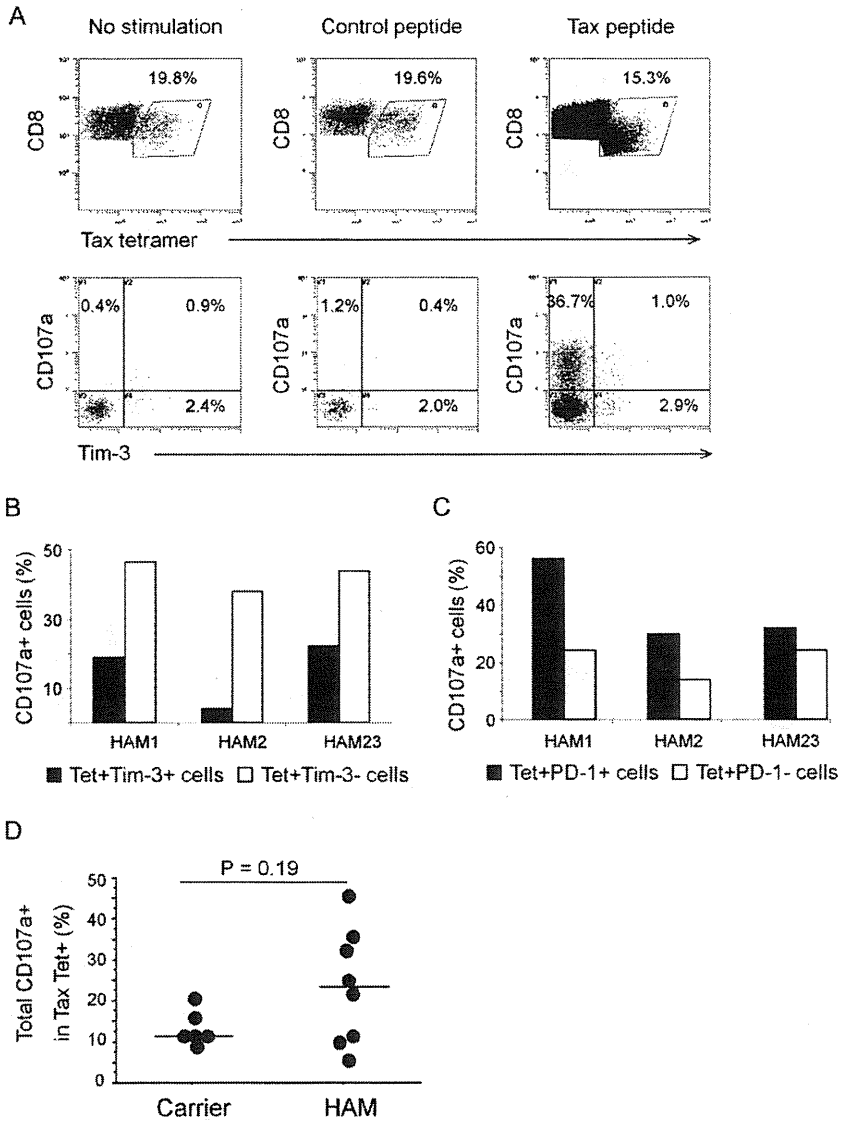

Figure 5. Reduced CD107a expression on Tim-3$^+$ HTLV-I Tax-specific CTLs. PBMCs from 8 HAM/TSP patients and 6 carriers were stimulated with HTLV-I Tax peptide or a control peptide, and cultured in the presence of an anti-CD107a antibody and brefeldin A for 4 hours. The expression of CD107a on CD8$^+$Tax tetramer$^+$ cells was analyzed. (*A*) Representative data from a HAM/TSP patient are shown. In the upper row, Tax peptide-stimulated Tax tetramer$^+$ cells show a parallel decrease in fluorescence intensity for CD8 and Tax tetramer. The same was not observed with the control peptide. The percentage of tetramer$^+$ cells is reduced after Tax peptide stimulation. In the lower row, the frequency of CD107a-expressing cells is analyzed in tetramer$^+$Tim-3$^+$ and tetramer$^+$Tim-3$^-$ cells. Tetramer$^+$Tim-3$^+$ cells show a lower percentage of CD107a$^+$ cells than tetramer$^+$Tim-3$^-$ cells. (*B*, *C*) Three HAM/TSP patients from whom more than 10^4 Tax-tetramer$^+$ cells could be collected were chosen for a precise evaluation. (*B*) The summary data show low CD107a expression in tetramer$^+$Tim-3$^+$ cells in comparison with tetramer$^+$Tim-3$^-$ cells, after background subtraction. (*C*) The summary data show high CD107a expression in tetramer$^+$ PD-1$^+$ cells in comparison to tetramer$^+$ PD-1$^-$ cells. (*D*) The percentage of CD107a$^+$ cells within Tax tetramer$^+$ cells from 8 HAM/TSP patients and 6 carriers is shown. No significant difference was observed in the percentage of CD107a$^+$ cells between the 2 groups ($P = .19$ by Mann–Whitney *U* test). The bars indicate the medians.

NOTE: PBMCs: peripheral blood mononuclear cells; HAM/TSP: HTLV-I–associated myelopathy/tropical spastic paraparesis; HTLV-I: human T-lymphotropic virus type I; CD107a: cluster of differentiation 107a; HAM: HTLV-I–associated myelopathy/tropical spastic paraparesis; Tet: tetramer.

CTLs from 8 HAM/TSP patients and 6 asymptomatic carriers. Representative data from a HAM/TSP patient are shown in Figure 5*A*. Specific antigen-induced CD107a expression was higher in tetramer$^+$Tim-3$^-$ cells than in tetramer$^+$Tim-3$^+$ cells. At the same time, CD107a expression was higher in tetramer$^+$PD-1$^+$ cells than in tetramer$^+$PD-1$^-$ cells from 3 HAM/TSP patients from whom we could collect more than 10^4 tetramer$^+$ cells for a more precise evaluation (Figures 5*B* and 5*C*).

Downloaded from http://jid.oxfordjournals.org/ at Kagoshima University on April 10, 2012

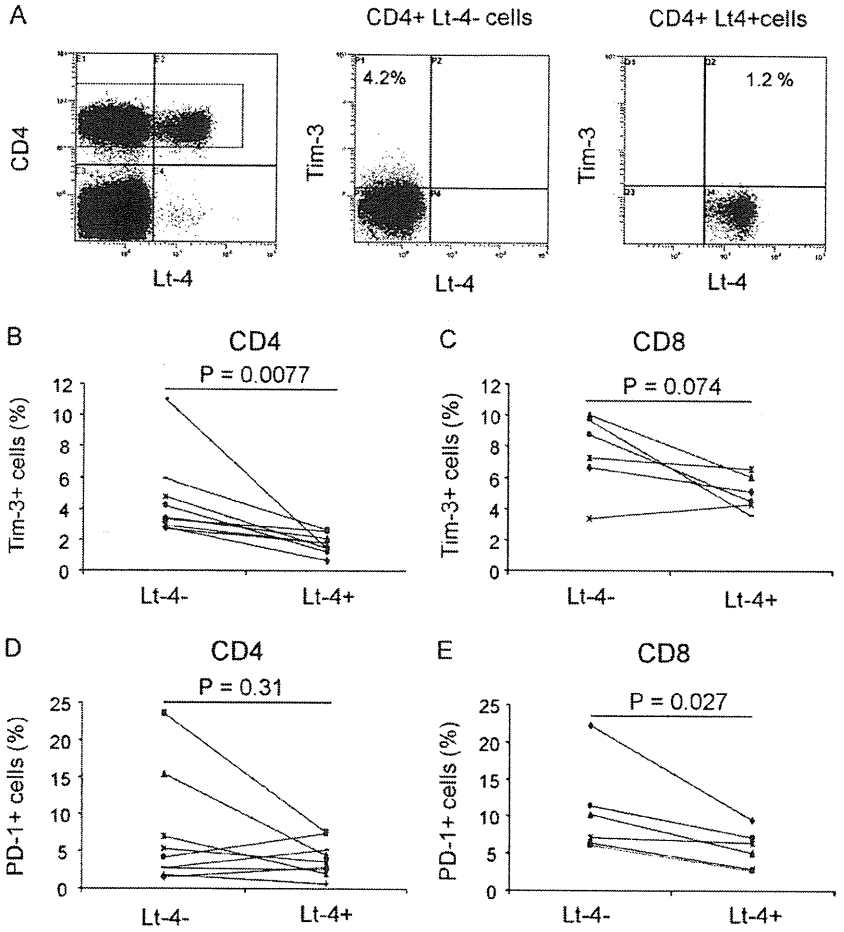

Figure 6. Low expression of Tim-3 on HTLV-I–infected cells. PBMCs from 9 HAM/TSP patients were cultured for 12 hours. Cells were double stained for the intracellular HTLV-I Tax protein, using the Lt-4 antibody, and the cell surface Tim-3 or PD-1. (*A*) After gating on $CD4^+$ cells, expression of Tim-3 was analyzed in either $CD4^+Lt\text{-}4^+$ or $CD4^+Lt\text{-}4^-$ cells. Representative data from a HAM/TSP patient show low percentage of $Tim\text{-}3^+$ cells in $CD4^+Lt\text{-}4^+$ cells in comparison to $CD4^+Lt\text{-}4^-$ cells. (*B, D*) Combined data from 9 HAM/TSP patients show significantly lower Tim-3 expression in $CD4^+Lt\text{-}4^+$ cells than in $CD4^+Lt\text{-}4^-$ cells. No significant difference in PD-1 expression between both groups was found by Wilcoxon signed-rank test. (*C, E*) Combined data from 6 HAM/TSP patients show that Tim-3 expression tended to be lower in $CD8^+Lt\text{-}4^+$ cells than in $CD8^+Lt\text{-}4^-$ cells and that PD-1 expression was significantly lower in $CD8^+Lt\text{-}4^+$ cells than in $CD8^+Lt\text{-}4^-$ cells, by Wilcoxon signed-rank test.

NOTE: PBMCs: peripheral blood mononuclear cells; HAM/TSP: HTLV-I–associated myelopathy/tropical spastic paraparesis; HTLV-I: human T-lymphotropic virus type I; Tim-3: T cell immunoglobulin and mucin domain-containing molecule-3; PD-1: programmed cell death-1.

Furthermore, when we reanalyzed the frequency or MFI of $CD107a^+$ cells within the Tax $tetramer^+$ cell population, we could not detect a significant difference between HAM/TSP patients and asymptomatic carriers (Figure 5*D*). Also, we could not detect a significant correlation between the frequency of $CD107a^+$ cells and HTLV-I proviral load (data not shown).

Low Expression of Tim-3 on $CD4^+$ HTLV-I–infected Cells

To assess Tim-3 expression on HTLV-I–infected cells, we cultured PBMCs from 9 HAM/TSP patients for 12 hours in order to induce the expression of the HTLV-I Tax protein [30]. After harvesting, Tax protein was simultaneously detected with Tim-3 or PD-1 (Figure 6*A*). We observed that Tim-3 expression was significantly lower in Tax^+ $CD4^+$ cells ($Lt\text{-}4^+$ cells) than in Tax^-CD4^+ cells ($P = .0077$ [Figure 6*B*]). On the contrary, we observed no significant differences in PD-1 expression between Tax^+CD4^+ and Tax^-CD4^+ cells ($P = .31$ [Figure 6*D*]). In addition, we assessed the expression of Tim-3 or PD-1 in infected $CD8^+$ cells from 6 cases that showed a reasonable percentage of infected $CD8^+$ cells. We found that Tim-3 expression tended to be lower in Tax^+CD8^+ cells than in Tax^-CD8^+ cells ($P = .074$ [Figure 6*C*]), whereas PD-1 expression was significantly lower in Tax^+CD8^+ cells than in Tax^-CD8^+ cells ($P = .027$ [Figure 6*E*]). No significant correlations were observed between the MFI of Lt-4–positive cells and the frequency or

Downloaded from http://jid.oxfordjournals.org/ at Kagoshima University on April 10, 2012